

# Baryon spectra and antiparticle-to-particle ratios from the improved AMPT model

Yuncun He<sup>1,2,\*</sup> and Zi-Wei Lin<sup>2,3,\*\*</sup>

<sup>1</sup>Faculty of Physics and Electronic Technology, Hubei University, Wuhan 430062, China

<sup>2</sup>Department of Physics, East Carolina University, Greenville, North Carolina 27858, USA

<sup>3</sup>Key Laboratory of Quarks and Lepton Physics (MOE) and Institute of Particle Physics, Central China Normal University, Wuhan 430079, China

**Abstract.** The current version of a multi-phase transport (AMPT) model with string melting can reasonably describe the  $dN/dy$  yields,  $p_T$  spectra and anisotropic flows of pions and kaons at low  $p_T$  in heavy ion collisions at RHIC and LHC energies, although it failed to reproduce the  $dN/dy$  and  $p_T$  spectra of baryons. In this work, we improve the quark coalescence mechanism in AMPT by removing the forced separate number conservations of mesons, baryons and antibaryons in each event. We find that the improved AMPT model can better describe the yields at midrapidity, the  $p_T$  spectra and elliptic flow of low- $p_T$  baryons in comparison with the experimental data. Antiparticle-to-particle ratios of strange baryons are also significantly improved.

## 1 Introduction

The original string melting version of AMPT [1], which converts all the excited strings to partons before parton cascade and hadronizes with the quark coalescence mechanism, could fit the elliptic flow and two-pion interferometry at RHIC very well, but it failed to reproduce the  $p_T$  spectra and rapidity distributions of hadrons. With a new set of key parameters, the string melting AMPT model was improved to reasonably reproduce the  $dN/dy$  yields,  $p_T$  spectra and elliptic flows of pions and kaons at low  $p_T$  in heavy ion collisions at  $\sqrt{s_{NN}} = 200$  GeV and 2.76 TeV [2]. It has also been used to predict the identified particles  $dN/dy$ ,  $p_T$  spectra, azimuthal anisotropies and longitudinal correlations in the Pb+Pb collisions at  $\sqrt{s_{NN}} = 5.02$  TeV [3]. However, it still has some deficiencies on baryon descriptions. It overestimates the proton yield at midrapidity and underestimates the slope of the proton  $p_T$  spectra significantly. In addition, the antiparticle-to-particle ratios from the current AMPT model are often above unity for strange baryons, contrary to naive expectations or the data.

The coalescence in the current AMPT model forces the numbers of mesons, baryons and antibaryons in an event to be conserved separately. The model first searches partners for quarks from the melting of mesons to form mesons, then searches partners for the remaining quarks or antiquarks to form baryons or antibaryons. In this study [4], we remove the artificial separate conservation of the numbers of mesons, baryons and antibaryons in each event; while the conservations of the net

---

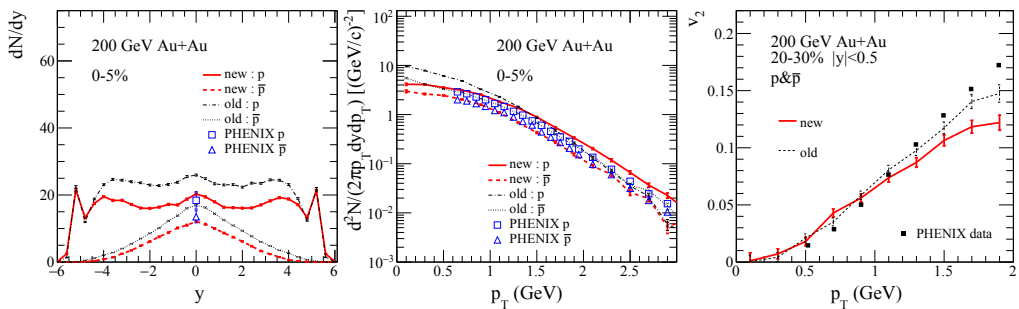
\*e-mail: [hyuncun@foxmail.com](mailto:hyuncun@foxmail.com)

\*\*e-mail: [linz@ecu.edu](mailto:linz@ecu.edu)

baryons and net strangeness are still satisfied. Each (anti)quark now has the freedom to form a meson or a (anti)baryon depending on the distances between the coalescing partners. A new constant parameter  $r_{BM}$ , which controls the relative probability of a quark forming a baryon versus a meson, is introduced and its value has been determined by fitting the experimental data [4]. However, note that in principle this parameter should be determined from the hadron wavefunctions. In this new AMPT model, we use the Lund string fragmentation parameters  $a = 0.55$  for Au+Au collisions at 200 GeV and  $a = 0.2$  for Pb+Pb collisions at 2.76 TeV respectively, and  $b = 0.15 \text{ GeV}^{-2}$  for both collisions. The relative production of strange to nonstrange quarks from Lund string fragmentation is still kept 0.4 and the strong coupling constant is set to  $\alpha_s = 0.33$  as in earlier studies [2, 3], while the parton cross section is set to 1.5 mb instead of 3 mb in those earlier studies.

## 2 Results for protons and antiprotons

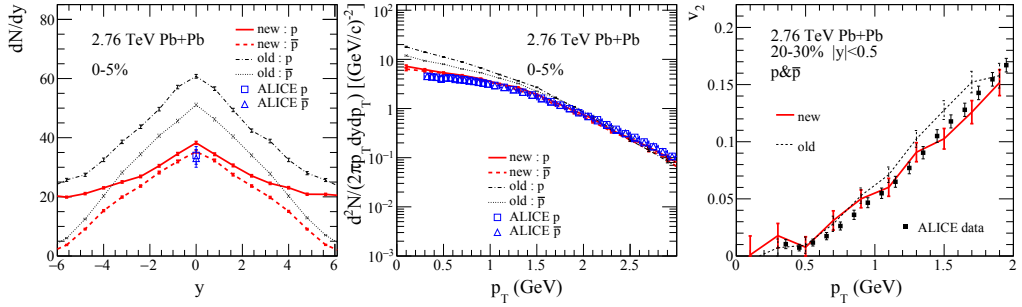
Figure 1 shows the rapidity distributions (left panel),  $p_T$  spectra at midrapidity (middle panel), and  $v_2$  as function of  $p_T$  (right panel) of protons and antiprotons in Au+Au collisions at 200 GeV. Figure 2 shows the results for Pb+Pb collisions at 2.76 TeV. The experimental data are from PHENIX [5, 6] and ALICE [7, 8] respectively, and both of them have included the corrections from weak decays. The thin curves represent results produced by the old quark coalescence, which gives higher yields at midrapidity (particularly at LHC) and too soft  $p_T$  spectra at both RHIC and LHC. The thick curves represent results produced by the new quark coalescence, which gives lower yields and harder  $p_T$  spectra and is thus more consistent with the data. The  $p_T$  dependence of  $v_2$  from the new coalescence shows little change; this is expected since the elliptic flow is a normalized variable. We have checked that the new model also reasonably describes the  $dN/dy$ ,  $p_T$  spectra and elliptic flow of low- $p_T$  pions and kaons. Thus the string melting AMPT model with the new quark coalescence provides a much better description of the bulk matter in high-energy heavy ion collisions.



**Figure 1.**  $dN/dy$ ,  $p_T$  spectra and  $v_2$  of protons and antiprotons from the new (thick curves) and old (thin curves) quark coalescence for Au+Au collisions at 200 GeV in comparison with the PHENIX data.

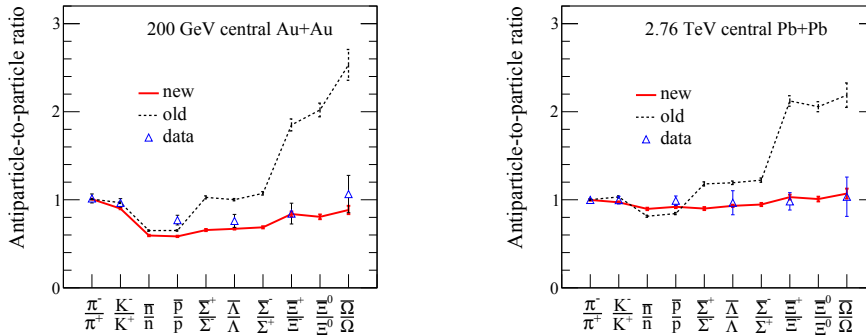
## 3 Results for antiparticle-to-particle ratios

Figure 3 shows the antiparticle-to-particle ratios of  $\pi^-/\pi^+$ ,  $K^-/K^+$ ,  $\bar{n}/n$ ,  $\bar{p}/p$ ,  $\bar{\Sigma}^+/\Sigma^-$ ,  $\bar{\Lambda}/\Lambda$ ,  $\bar{\Sigma}^-/\Sigma^+$ ,  $\bar{\Xi}^+/\Xi^-$ ,  $\bar{\Xi}^0/\Xi^0$  and  $\bar{\Omega}/\Omega$  around midrapidity for central Au+Au collisions at 200 GeV (left panel) and Pb+Pb collisions at 2.76 TeV (right panel) in comparison with the experimental data [7, 9–13]. We see that the results from the new quark coalescence (solid curves) are generally more consistent with the experimental data than results from the old quark coalescence (dashed curves). In particular, the



**Figure 2.**  $dN/dy$ ,  $p_T$  spectra and  $v_2$  of protons and antiprotons from the new (thick curves) and old (thin curves) quark coalescence for Pb+Pb collisions at 2.76 TeV in comparison with the ALICE data.

antiparticle-to-particle ratios of multi-strange baryons  $\bar{\Xi}^+/\Xi^-$ ,  $\bar{\Xi}^0/\Xi^0$  and  $\bar{\Omega}^+/\Omega^-$  are much lower than before and now agree well with the data. We also see that the new ratios at 2.76 TeV are closer to unity than those at 200 GeV, since baryons and antibaryons are more symmetric in higher energy collisions.



**Figure 3.** Antiparticle-to-particle ratios around midrapidity from the new (solid curves) and old (dashed curves) quark coalescence for Au+Au collisions at 200 GeV and Pb+Pb collisions at 2.76 TeV in comparison with data.

Figure 4 shows the antibaryon-to-baryon ratios around midrapidity in central collisions as functions of energy, including the results for Au+Au collisions at 62.4 GeV, 130 GeV, 200 GeV and Pb+Pb collisions at 2.76 TeV and 5.02 TeV. Note that we have used the Lund string parameter  $a = 3.2$  for 62.4 GeV and  $a = 1.65$  for 130 GeV. We see that the results from the new quark coalescence (left panel) are generally more consistent with the experimental data than the old results (right panel), especially for the ratios of multistrange baryons. Overall, the ratios from the new quark coalescence for all these baryons gradually approach unity as the colliding energy increases, as we would expect.

The new quark coalescence is much more physical, however some problems still exist. For example, the antiproton-to-proton ratios are well below the data at RHIC and LHC as shown in Figure 3. Further improvements, such as the implementation of energy-momentum conservation in quark coalescence, may be necessary.

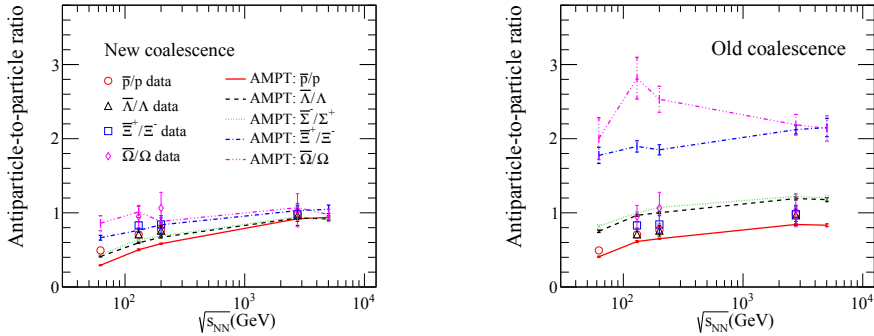


**Figure 4.** Antibaryon-to-baryon ratios around midrapidity as functions of collision energies from the new (left panel) and old (right panel) quark coalescence in comparison with data.

## 4 Conclusion

We have improved the quark coalescence component in the string melting version of a multi-phase transport model AMPT. In particular, we have removed the artificial separate conservation of the numbers of mesons, baryons, and antibaryons in an event, where only the conservation of the net-baryon number in an event is needed for the coalescence process. In the new quark coalescence, a quark now has the freedom to form either a baryon or a meson, depending on the distance to its coalescence partner(s). We have compared the results with the experimental data and shown that the new model can reasonably describe the  $dN/dy$ ,  $p_T$  spectra, and  $v_2$  of pions, kaons, and most (anti)baryons. Significant improvements are also made on the antibaryon-to-baryon ratios of  $\Xi$  and  $\Omega$ .

We thank support from the NSFC of China under Grants No. 11628508, No. 11547016 and No. 11447190.

## References

- [1] Z. W. Lin, C. M. Ko, B. A. Li, B. Zhang and S. Pal, Phys. Rev. C **72**, 064901 (2005)
- [2] Z. W. Lin, Phys. Rev. C **90**, no. 1, 014904 (2014)
- [3] G. L. Ma and Z. W. Lin, Phys. Rev. C **93**, no. 5, 054911 (2016)
- [4] Y. He and Z. W. Lin, Phys. Rev. C **96**, no. 1, 014910 (2017)
- [5] S. S. Adler *et al.* [PHENIX Collaboration], Phys. Rev. C **69**, 034909 (2004)
- [6] A. Adare *et al.* [PHENIX Collaboration], Phys. Rev. C **93**, no. 5, 051902 (2016)
- [7] B. Abelev *et al.* [ALICE Collaboration], Phys. Rev. C **88**, 044910 (2013)
- [8] B. B. Abelev *et al.* [ALICE Collaboration], JHEP **1506**, 190 (2015)
- [9] J. Adams *et al.* [STAR Collaboration], Phys. Rev. Lett. **98**, 062301 (2007)
- [10] C. Suire [STAR Collaboration], Nucl. Phys. A **715**, 470 (2003)
- [11] B. I. Abelev *et al.* [STAR Collaboration], Phys. Rev. C **79**, 034909 (2009)
- [12] S. Schuchmann, Ph.D. thesis, Goethe University Frankfurt, 2015
- [13] B. B. Abelev *et al.* [ALICE Collaboration], Phys. Lett. B **728**, 216 (2014) Erratum: [Phys. Lett. B **734**, 409 (2014)]